Spectroscopic effects of negative and positive stresses on the transition-metal-ion activated sapphire fibers

KI-SOO LIM

OPTICS LABORATORY
KOREA STANDARDS RESEARCH INSTITUTE

ABSTRACT

The spectroscopic properties of Cr^{3+}-doped sapphire and Ti^{3+}-doped sapphire fibers are reported. Tensile stress produces blue shifts of the R lines and changes in their radiative lifetimes and integrated intensities which can be correlated to stress-induced changes of the crystal-field parameters in a Cr^{3+}-doped sapphire fiber. A net red shift of the zero phonon fluorescence line of ^2Eg state and a decrease of the splittings of ^2T_2g state with uniaxial stress are observed in a Ti^{3+}-doped sapphire. In excitation spectra the two peaks from the ^2Eg state are shifted to the blue with different rates. The changes are attributed to the stress-induced changes of crystal field and Jahn-Teller effect.

1. Introduction

Several piezospectroscopic studies of transition-metal ions in crystals have been published[1,2]. Specially, ruby (Cr^{3+}:Al_2O_3) is an extremely-well- studied material, owing to its use in lasers and as a high-pressure standard in diamond-anvil cells[3]. As some Cr^{3+}-doped crystals which have low crystal field have recently been studied as the active lasing materials, the pressure dependence of the Cr^{3+} ion emission spectrum in various hosts is of interest[4,5]. Although the effects of hydrostatic pressure or uniaxial compressive stress on the R lines have been investigated, the complementary effect of a stretching or tensile (negative) stress on the optical properties of transition-metal-ion activated solids has not been considered. This is principally because of experimental difficulties encountered in the stretching of bulk crystalline samples. The difficulties have been alleviated by the recent availability of single-crystal fibers[6].

Ti^{3+} doped sapphire has been of interest in recent yearts due to its potential as a material for tunable solid state lasers[7]. The lasing transition involves the excited state ^2Eg and the ground state ^2T_2g, both of which are Jahn-Teller distorted[8]. Thus, the Jahn-Teller effect is expected to influence the lasing performance in a fundamental way[9].

In this report, the results of spectroscopic studies of the effects of negative stress on the R lines of Cr^{3+} and positive stress on the spectra of Ti^{3+} in sapphire crystal fibers are presented.

2. Experimental

2.1 Cr^{3+}-doped sapphire

The fibers used in the study were grown using the laser-heated pedestal growth(LHPG) method at Stanford University[6]. The fiber for stretching is nominally pure sapphire. It is generally difficult, however, to exclude Cr contamination entirely from raw sapphire. The sample used produced sufficient luminescence from the trace impurities to allow to conduct the investigation. The fiber has a diameter of 163 μm and a length of 2 cm. It showed the characteristics of a twinning structure along the fiber axis in the X-ray diffraction, optical polarization and the Raman scattering measurements. It can be concluded that the c axes of the twins make an angle of 20 to 30 ° with the fiber axis. The ESR studies indicate that the unintentional Cr^{3+} doping level of the fiber is less than 10^{15} spins/cm^3.

Tensile stress was applied to the sample along the fiber axis using a specially designed sample holder, which kept the optical alignment of the fiber versus the analyzing spectrometer stable when changing the stress. Tensile stress was applied using calibrated weights. The experiments reported here were all conducted by 514.5-nm cw Ar-laser light; laser heating, which leads to red shifts of the R lines, was found to be negligible as determined by the R-line positions when the fiber was excited with no stress. Figure 1 shows the shift of the R lines as a function of tensile stress. Results from uniaxial stress experiments [11] are also shown for comparison. Instead of a red shift, the R lines now evince a linear blue shift as a function of increasing stretching or tensile stress; the linearity of this dependence breaks down in the vicinity of 6.0 kbars, the yielding point. The fiber broke at 7.7 kbars: this is, of course the tensile strength of the sapphire fiber. Our value is larger than the value of 4.2 kbars reported in the literature for bulk material. The latter value depends on the quality of the sample, thus a higher value implies a better crystal.

2.2. Ti^{3+}-doped sapphire

The sample used in these studies is doped with 0.1 wt% Ti^{3+}. The fiber has a diameter of 850 μm. The Ar 514.5 nm laser line was used to excite the ^2Eg state, and a double spectrometer (SPEX 1401) of spectral resolution 0.2 cm^{-1} was employed to analyze the fluorescence signal. For excitation measurements, a tungsten halogen lamp and a 30-cm monochromator system with a spectral resolution of 0.5 nm were used as the monochromatic light source. The analyzer was set at 14100 cm^{-1}. All the experiments were done at 10 K using a refrigerator.

In order to keep the symmetry of the crystal unchanged stresses were applied parallel to the axis of the sapphire fiber. The fiber axis was found to be coincident with the c axis of the crystal a fact which was confirmed using Raman scattering studies.

Figure 2(a) shows the stress device designed for optical studies at low temperature; it is capable of reaching 20 kbar. The stress is produced by the stressing screw and the elastic metal plate and transmitted onto the sapphire fiber and the ruby cube through the metal cylinder and the metal spacers. The laser beam excites the sample transversely and hence is perpendicular to the fiber axis (the c axis) and to the applied stress. The R line shift of a ruby sample was used to calibrate the stress as in the case of hydrostatic pressure experiments.

The R line shift rate as a function of hydrostatic pressure is a simple sum of the three shift rates by uniaxial stresses along the a, b, and c axes, respectively[10]. Thus, the conclusion that the absolute shift rates of the R line under hydrostatic pressure do not depend on temperature in a range from 4.2 to 300 K also applies to the case of the uniaxial stress. An R line shift rate of 0.182 cm^{-1}/kbar with stress parallel to the c axis of ruby, derived from Feher and Sturge's data at 77 K [11], was used to calibrate the stress in this work at all temperatures.

For example, Fig. 2(b) shows the R_1 lines of ruby at zero and 4 kbar of uniaxial stress. The line shift is defined as the shift of the center of the zero field splittings. $(R'_1 - R''_1)/2$.

3. Results and Discussion

3.1. Negative stress effects in a Cr^{3+} doped sapphire

For Cr^{3+} in sapphire, the energy of the ^2E states is determined by the Racah coefficients B and C. The latter are electrostatic in nature and are related to the overlap integral of the covalent bond connecting the 3d orbital of Cr^{3+} with the p orbital of O^{2-}. Compressive stress or hydrostatic pressure increases the overlap of these radial wave functions, which in turn reduces the value of the Racah coeffficients.[12] The net result is a decrease of the ^2E energy and a red shift of the R lines. With tensile strength, the opposite effect is to be expected; i.e., any expansion of the lattice increases the B and C values, and a blue shift results. The fact that the rate of the stress and the pressure-induced shifts of the ^2E level center of gravity, 0.200, 0.215, and 0.757 cm /kbars for tensile, compressive,[11] and hydrostatic[12] pressure, respectively, are of the same order of magnitude is simply a consequence of their common origin.

On the other hand, the R_1-R_2 splitting originates from an interplay of the small trigonal field components and the spin-orbit coupling. For ruby this separation of 29 cm^{-1} is directly related to the trigonal parameters ν and ν' [11,13]; the latter consist of one-electron matrix elements of the trigonal field within the t^2 and between the t^2 and e configurations, respectively. [16] Generally ν' is small and is neglected in the lowest-order

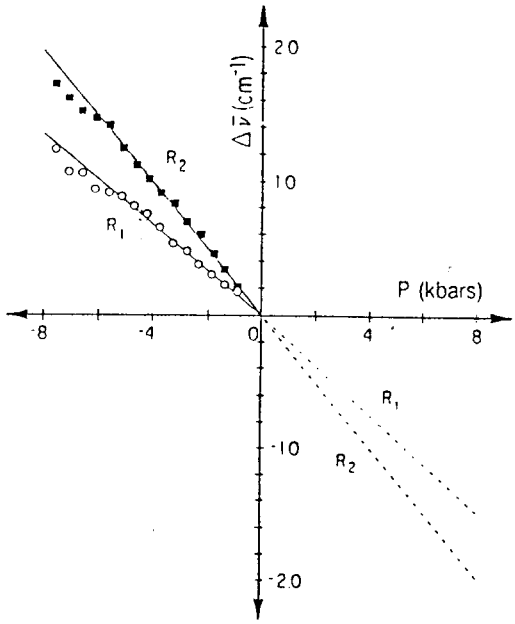

Fig. 1. Tensile stress dependence of the blue shift of the R lines of Cr in a single crystal sapphire fiber. As can be seen, the shifts are linear up to the yielding point of 6.0 kbars; the tensile strength of the fiber is 7.7 kbars. Shifts arising from uniaxial compression stress are also shown for comparison.

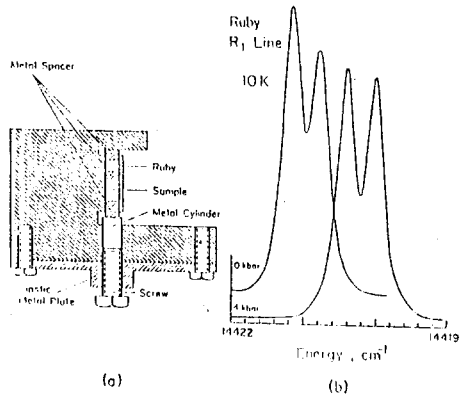

Fig. 2. (a) The stress device; (b) The R lines of a ruby sample for stress calibration at 10 K.

approximation, thus the splitting can be expressed as $\Lambda = 4\zeta\nu/3\Delta$ [11] where ζ is the spin-orbit coupling parameter and Δ is the ^2E-$^2T_2$ separation. In principle, the value of ν and its stress dependence may be calculated. It suffices here to say that stresses applied parallel and perpendicular to the c axis of sapphire yield contributions of different signs to the value of $\delta\nu$. In the case of uniaxial compressive stress applied parallel to the optic axis, $\delta\nu$ is negative, whereas perpendicular stress gives a positive value. The converse is true for tensile stress; however, the canting of the c axis in our sample combines stresses in both directions with the positive contribution from the parallel component dominating. From the estimated canting angle, the rate of splitting of the 2A-E levels under parallel tensile stress can be calculated to be 0.109 ± 0.017 cm^{-1}/kbars.

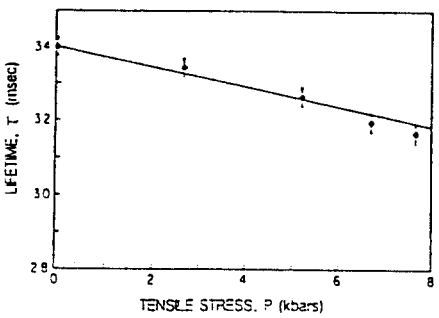

Fig. 3. Radiative lifetime of the R line (^2E to $^4A_2$) transitions of Cr^{3+} in the optical fiber shown as a function of applied tensile stress. The solid line is a theoretical fit to the observed decrease as discussed in text.

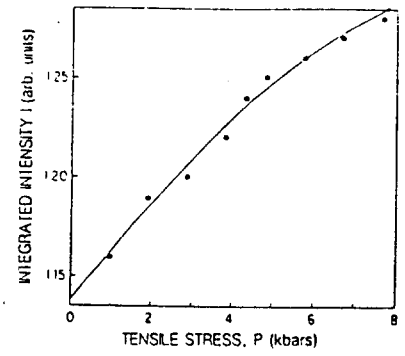

Fig. 4. Changes in the integrated total intensity of the R lines in a sapphire fiber as a function of decompressing stress. This change is connected to the variation of the energy separation of the ^2E from the $^4T_2$ states of Cr^{3+}.

The radiative lifetime of the ^2E state of the fiber was also investigated. Figure 3 shows the stress dependence of the lifetime of the transition at room temperature. In view of the extreme dilution of our sample, interionic effects related to radiative or nonradiative transfer processes are too weak to be observed. Therefore, we believe that decrease in the lifetime with increasing stress depicted in the Fig. 3 arises from changes in the transition probability.

The electric-dipole transition strength is given by [16]

$$I(^2E - {}^4A_2) = | \hat{R}/W(^4T_2) - W(^2E) |^2 , \qquad (1)$$

where

$$\hat{R} = \sum_x C_x \langle {}^4A_2 | e\hat{r} | {}^4T_2x \rangle \langle {}^4T_2x | \zeta \hat{L}\hat{S} | {}^2E \rangle . \qquad (2)$$

In Eq. (2), the x's stand for the orbital components of the $^4T_2$ states. In our case, the applied decompression reduces Dq, the crystal-field strength parameter, resulting in a decrease of the ^2E to $^4T_2$ energy separation, the denominator in Eq.(1). The net effect is an increase in I. An increase in the total intensity of the R lines with increasing tensile stress was also observed in our experiments and is summarized in Fig. 4.

The lifetime can be written as

$$\tau = \frac{\tau_o}{1 - \eta_o + \eta_o(1 + kP)^{-2}} , \qquad (3)$$

where η_o and τ_o are the fluorescence quantum efficiency and the lifetime with zero stress, respectively, P is the applied stress (negative for tensile stress, in kilobars), and k is the specific rate of relative shift of the ^2E to $^4T_2$ energy separation and is defined as

$$k = \frac{\Delta [W(^4T_2) - W(^2E)]}{[W(^4T_2) - W(^2E)]P} . \qquad (4)$$

In Fig. 3, the solid line shows a theoretical least-squares fit to the lifetime data with parameters η_o = 0.73,[15] τ_o = 3.4 msec, and k = 5.6 x 10^{-3}. From the latter k value, and taking $W(^4T_2) - W(^2E)$ = 2330 cm^{-1},[2] the ^2E to $^4T_2$ separation is estimated to change 100 cm^{-1} at 7.7 kabrs, in good agreement with Ref. 2.

3.2. Effects of uniaxial stress on the excited state ^2Eg of Ti^{3+}

The $^2D(3d^1)$ energy level of free Ti^{3+} ions is spkit into ^2T_2g and ^2Eg states in the cubic crystal field of oxygen octahedrons of sapphire. The ground state ^2T_2g is further split into three Kramer's doublets $_2E_{1/2}$ $_1E_{1/2}$ and $E_{3/2}$ by the trigonal field component and spin-orbit coupling [8]. Although spin-orbit coupling, in combination with the trigonal field, may split has excited state ^2E, the splitting of the band is probably too small to measure. However, the static Jahn-Teller effect in this state produces two lattice-distorted states, $E_{1/2}$ and $E_{3/2}$, with a splitting ~3000 cm^{-1}. The fluorescence emission observed at low temperatures

results from a transition from the lower Jahn-Teller state $E_{3/2}(^2Eg)$ to the ground state ^2T_2g [9].

With no stress, the three zero-phonon lines R_1, R_2, and R_3 of the fluorescent transitions, peaking at 16.220.5, 16183.5 and 16114.5 cm^{-1} with linewidths 10, 10.5 and 16 cm^{-1}, respectively, are shown in Fig. 5 also shown is the corresponding spectrum recorded at 17 kbar. In each case, their accompanying single-phonon sideband structures are also shown in the figure. In Fig. 6 the linear red shift of the zero-phonon R_1 line $[E_{3/2}(^2Eg) \rightarrow E_{3/2}(^2T_2g)]$ is plotted as a function of increasing stress. The rate of the red shift is calculated to be 0.43 cm^{-1}/kabr. The excitation spectra (absorption) corresponding to the transition $^2T_2g \rightarrow {}^2Eg$ at zero and 17 kbar are shown in Fig. 7. The spectra consist of two broad overlapping bands from the Jahn-Teller components, peaking at 20480 and 17990 cm^{-1} with zero stress. These bands are shifted to 20570 and 18060 cm^{-1} at 17 kbar, respectively. The measured blue shift rates are 5.2 and 4.1 cm^{-1}/kbar.

In general, the pressure/stress-induced shift of electronic transition energy in solid aries from two sources, i.e., changes in crystal field and relative changes in the strength of electron-phonon (lattice) interaction. The size of the effects depends on the given crystalline system. When dealing with broadband or phonon assisted transitions, the field and coupling changes play equal roles. In addition, for the Jahn-Teller system, the pressure/stress effects can be more complicated since the Jahn-Teller interaction strength may also be dependent on pressure/stress. The static Jahn-Teller effect can be intensified by stress due to increases in covalency and in the strength of the electron-phonon interaction. The interplay of these two interactions, i.e., crystal field and Jahn-Teller effect, can be identified as the source of the red shift for the zero-phonon line (Figs. 5 and 6). These considerations may be summarized schematically as depicted in Fig. 8. In the figure, the dashed and solid lines describe the configuration coordination diagrams of electronic states ^2Eg and ^2T_2g with and without stress, respectively. The valley of the upper Jahn-Teller level $E_{1/2}(^2Eg)$ is shifted upward under stress due to the increased cubic field; however, the minimum of the lower Jahn-Teller level, $E_{3/2}(^2Eg)$, is depressed in energy due to an overcompensation of the field increase by the increased Jahn-Teller energy. On the other hand, according to DFS theory [14], stress can change the coupling of electronic states to the lattice, and the equilibrium point or origin of the configuration coordination will be shifted horizontally as shown in Fig. 8. The blue shift of the broad phonon-assisted absorption bands in Fig. 7 is therefore, a combined effect of these three processes: the increase of the cubic field component, the increased Jahn-Teller splitting and the shift of the vibronic configuration coordination. In addition, to a blue shift in absorption, a red shift of the phonon-assisted fluorescence is then also expected from Fig. 8. Such a red shift of broad band fluorescence from Ti^{3+} is also observed experimentally: a net shift of 65 cm^{-1} at 17 kbar was measured for the peak. If the average energy, 19235 and 19315 cm^{-1}, of the two absorption peaks in Fig. 4 are taken as the energy of ^2Eg (i.e., the energy gap Δ mentioned in the following) at zero stress and at 17 kbar respectively, a blue shift rate 4.7 cm^{-1}/kbar, of ^2Eg with stress can be deduced. Taking into account the red shift rate of the zero-phonon line, 0.42 cm^{-1}/kbar the static Jahn-Teller stabilization energy can be estimated to increase with a rate of 10.2 cm^{-1}/kbar.

Minomura and Drickamer [15] have measured the effects on the absorption of Ti^{3+} : Al_2O_3 under hydrostatic pressure. They reported a blue shift for the two absorption peaks with shift rates of 9.6 and 8.6 cm^{-1}/kbar for the upper and lower energy levels, respectively. Considering the difference in the experimental conditions, the result is consistent with theirs.

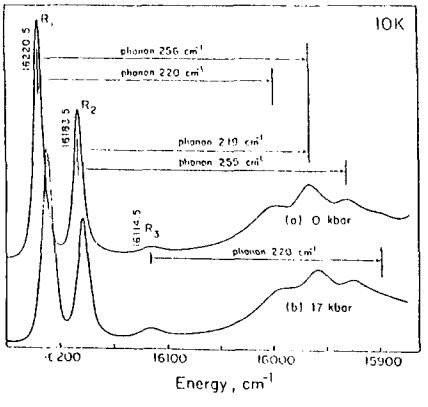

Fig. 5. The zero-phonon lines of the electronic transition $^2Eg \rightarrow {}^2T_2g$ for Ti^{3+} ions in sapphire fibers with their single-phonon sideband under zero and 17 kbar stress at 10 K.

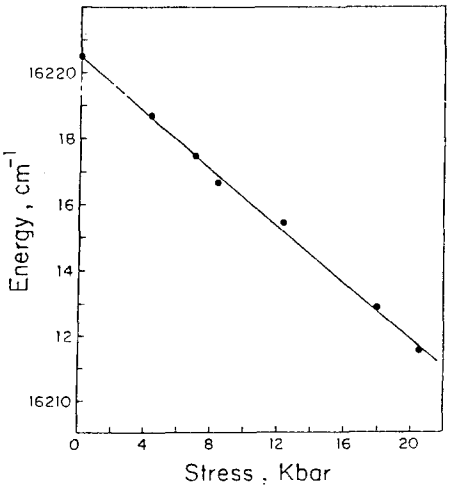

Fig. 6. Stress dependence of the energy of the zero-phonon electronic transition $E_{3/2}(^2Eg) \rightarrow E_{3/2}(^2T_2g)$ for Ti^{3+} ions in sapphire fibers at 10 K.

3.3. Stress effect on the splittings of $^2T_{2g}$

Figure 9 shows the stress dependence of the splittings of the ^2T_2g ground state. With increasing compressive stress along the c axis, the spin-orbital splting δ_1 and the trigonal field splitting δ_2 decreased nonlinearly.

As in other transition metal ions, the trigonal field component and the spin-orbital coupling predict much larger splittings than the observed values. The dynamic Jahn-Teller effect (the Ham effect), however, is known to quench the orbital angular momentum and reduce the splittings [8].

In Al_2O_3 Ti^{3+} ions are situated within an octahedron of oxygen atoms, which is elongated along the c axis, resulting in a trigonal field component. A compressive stress along the c axis will reduce this distortion and reduce the trigonal splitting δ_2. The stress-induced increase of the dynamic Jahn-Teller effect can further reduce the splitting δ_2 by increasing the quenching effect: a similar quenching of δ_1 is also expected. The changes of the observed splittings are again a combined effect of both interactions, i.e., the changes in trigonal field and Jahn-Teller quenching.

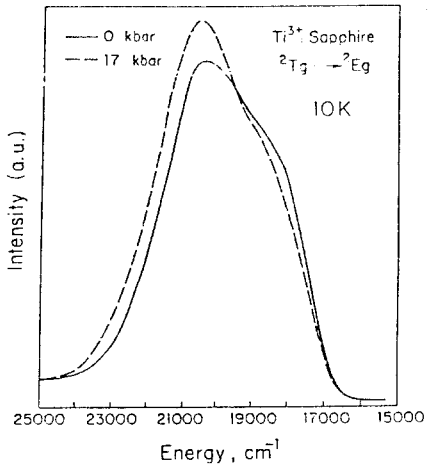

Fig. 7. The excitation spectra from ^2T_2g to ^2Eg for Ti^{3+} ions in sapphire fiber under zero and 17 kbar stress at 10 K.

4. Conclusion

The blue shift of R lines in a Cr^{3+}-doped fiber is explained by the decrease in the overlap of the covalent bond between the Cr^{3+} and O^{2-} ions. The increase of R_1-R_2 splitting originates mainly from the trigonal field parameter v. The radiative lifetime and the separation between ^2E and $^4T_2$ can be expressed as a function of the uniaxial stress. For the Ti^{3+}-doped sapphire a net red shift of the zero-phonon fluorescence line is the consequency of the combination of the increased cubic field and static Jahn-Teller energy. The ground state splittings decrease as a combined effect of the decreased spin-orbital coupling and the off-diagonal trigonal field parameter v', as well as the increase of the dynamic Jahn-Teller energy.

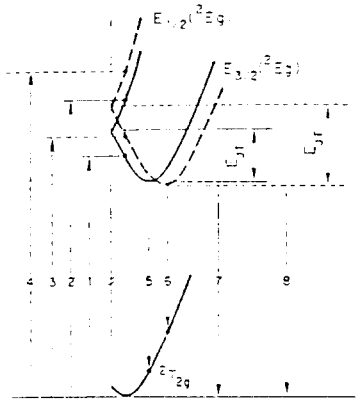

Fig. 8. Schematic diagram of the configuration coordinations and the corresponding optical transitions between the ^2T_2g and ^2Eg states of Ti^{3+} ions in sapphire fibers. Dashed lines represent the changes incurred under stress. The ground state splittings are not shown in the figure. The corresponding numbered transitions are as follows: 1,2 and 3,4: phonon-assisted absorptions without and with stress: 5 and 6: phonon-assisted emissions without and with stress: 7 and 8: zero- phonon transitions without and with stress, respectively.

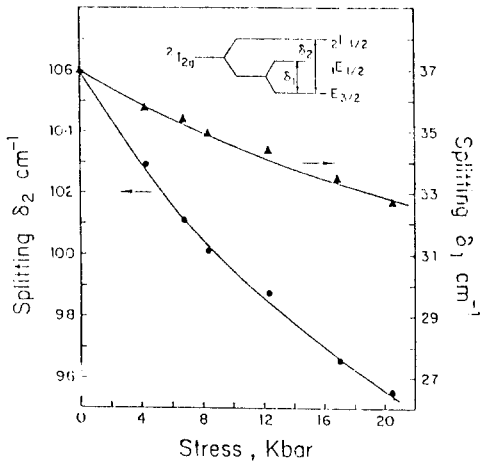

Fig. 9. Stress dependence of the splittings, δ_1 and δ_2 of the ground state manifold of Ti^{3+} ions in sapphire fibers at 10 K.

References

1. A. L. Schawlow in Advances in Quantum Electronics, J. R. Singer, ed. (Columbia U. Press, New York, 1961), Vol. 2, p. 50; A. L. Schawlow, A. H. Piksis, and S. Sugano, Phys. Rev. 122, 1469 (1961); L. F. Mollenauer and A. L. Schawlow, Phys. Rev. 168, 309 (1968).

2. A. A. Kaplyanskii and A. K. Przhevuskii, Sov. Phys. Dokl. 7, 37 (1962); Phys. Status Solidi 11, 629 (1965).
3. R. A. Forman, G. J. Piermarini, J. D. Barnett and S. Block, Science 176, 284 (1972).
4. T. Kottke and F. Williams, Phys. Rev. B 28, 1923 (1983).
5. J. F. Dolan, L. A. Kappers, and R. H. Bartram, Phys. Rev. B 33, 7339 (1986).
6. R.S. Feigelson, J. Cryst. Growth 79, 669 (1986)
7. P. Moulton, Opt. News 8, 9 (1982).
8. R. M. Macfarlane, J. Y. Wong and M. D. Sturge, Phys. Rev. 166, 250 (1968).
9. P. Albers, E. Stark and G. Huber, J. Opt. Soc. Am. B3, 134 (1986).
10. H. Liu, K. S. Lim, W. Jia, W. M. Yen, A. M. Buoncristiani and C. E. Byvik, Opt. Lett. 13, 931 (1988).
11. E. Feher and M. D. Sturge, Phys. Rev. 172, 244 (1968).
12. S. Sugano, in Lasers, Spectroscopy and Ideas, W. M. Yen and M. D. Levenson, eds., Vol. 54 in Springer Series in Optical Sciences (Springer- Verlag, New York, 1987), p. 224.
13. R. M. Macfarlane, Phys. Rev. 158, 252 (1967).
14. H. G. Drickamer, C. W. Frank and C. P. Siichter, Proc. Nat. Acad. Sci. USA 69, 933 (1972), Phys. Rev. B22, 4097 (1980).
15. S. Minormura and H. G. Drickamer, J. Chem. Phys. 35, 903 (1961).
16. S. Sugano, Y. Tanabe, and H. Kanimura, "Multiplets of Transition Metal Ions in Crystals" (Academic, New York, 1970).